Patchworking on Real Algebraic Curves

A Combinatorial Analogue of Real Algebraic Varieties

ZHANG Chencheng

May 12, 2022

Department of Mathematical Sciences
Shanghai Jiao Tong University

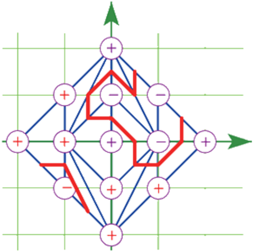

Content

Objectives

Our main objective is to present a combinatorial analogue of a special kind of real algebraic curve called **patchworking** [6], which provides the topology of these polynomials with real varieties.

Here we mainly focus on unary and binary polynomials.

Outline

- Dequantisation of real algebraic geometry on **logarithm paper**.
- Introduce the method of **patchworking**, which combines the real algebraic geometry with geometric combinatorics.
- Introduce **the first part of Hilbert's 16th problem**, and provide a counterexamples to the *Ragsdale Conjecture*.

Logarithm Paper of Polynomials

Visualising zeros of polynomial $a(x, y)$ on $\log\log$ paper

In order to visualise an real algebraic curve, we mainly focus on its **asymptotic behaviour**. The $\log\log$ paper is utilised for linearisation of a certain real algebraic curve on quadrants. The $\log\log$ paper is the diffeomorphism given by

$$\text{an open quadrant} \to \mathbb{R}^2, \quad (x, y) \mapsto (u, v) := (\log|x|, \log|y|). \tag{1}$$

E.g., the $\log\log$ paper of a real cubic curve is presented in **Figure 1**.

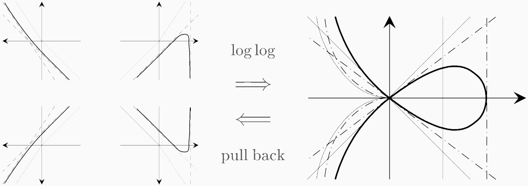

Figure 1: The $\log\log$ paper of $a(x, y) = 8x^3 - x^2 + 4y^2$.

Visualising polynomial $y = p(x)$ on $\log\log$ paper

For simplicity, we settle for polynomials in forms of $a(x, y) = y - p(x)$ with $y = p(x) = \sum_{k=0}^{n} a_k x^k$ as the set of zeros. The behaviour of $y = p(x)$ is determined by each monomials $\{a_k x^k\}_{k=0}^{n}$, that is, the preimage of asymptomatic lines in the $\log\log$ paper.

How $\log\log$ paper controls $y = p(x)$

The $\log\log$ paper manifests the *piece-wise* asymptomatic behaviour, especially in the vicinity of axes and at infinity, as **Figure 2** shows.

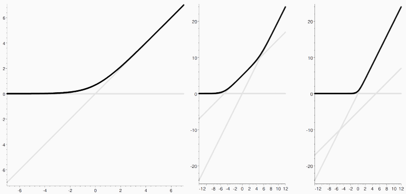

Figure 2: The $\log\log$ paper of $y = 1 + x^2$ and $y = 1 + e^{\pm 5}x + x^2$ in Q_{++}.

Control the set of zeros with maximum of monomials

For a unary polynomial $p(x) = \sum_{k=0}^{n} a_k x^k$, we consider the case that $a_k = e^{b_k} > 0$ for each $k = 0, 1, \dots, n$ and the truncation of its plot in $(x, p(x)) \cap Q_{++}$. Let Γ_p denotes the graph of

$$L_p(u) = \ln\left(\sum_{k=0}^{n} e^{ku+b_k}\right). \tag{2}$$

We define the function of maximal monomial

$$M_p(u) = \max_k \{ku + b_k\}_{k=0}^{n}, \tag{3}$$

which is piecewise linear. It is clear that

$$L_p(u) \leq M_p(u) = L_p(u) + R(u), \tag{4}$$

for some bounded and $+\infty$-vanishing function $R(u)$.

Maslov Dequantisation

RESCALING MAP OF $y = p(x)$

When we consider the *rescalings* $(u, v) \mapsto (Cu, Cv)$ for large $C > 0$, it follows that the graph $y = ax^k \Leftrightarrow v = ku + b$ becomes

$$v = ku + b \cdot C \Leftrightarrow y = a^C x^k. \tag{5}$$

Let $h = \dfrac{1}{C} > 0$, $p_h(x) = \sum_{k=0}^{n} a_k^{1/h} x^k$, and Γ_f^h be the graph Γ_p under the change of coordinates $(u, v) \mapsto (hu, hv)$.

It is clear that $\Gamma^h_{M(p_h)}$ doesnot depend on h. Thus $\lim_{h\to 0} \Gamma^h_{p_h} = \Gamma_{M(p)}$ in the C^0 sense. E.g., **Figure 3**.

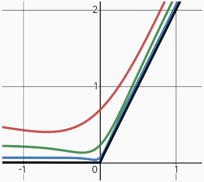

Figure 3: The limit $v = h\ln(e^{2u/h} - 2e^{u/h} + 2)$ as $h \to 0$ in C^0 sense.

The idea of Maclov Dequantisation

Consider a bunch of homomorphisms[1] with index $h \in [0, +\infty)$

$$D_h : \mathbb{R}[x_1, \dots, x_n] \to \{\log\log \text{ papers}\}, p \mapsto \Gamma^h_{p_h}, \quad x_i \mapsto h \ln x_i. \tag{6}$$

Then $D_h(a+b) = D_h(a) \oplus_h D_h(b)$, $D_h(a \cdot b) = D_h(a) \odot_h D_h(b)$.

From the perspective of Maslov [5], we shall construct a set of semirings $\{(S_h(=\mathbb{R}), \oplus_h, \odot_h)\}_{h \in [0,\infty)}$. Then $\odot_h$ is $+$ in normal sense, and

$$a \oplus_h b = \begin{cases} h \ln(e^{a/h} + e^{b/h}) & h > 0, \\ \max\{a, b\} & h = 0. \end{cases} \tag{7}$$

Established by Maslov, the theory *idempotent analysis* [3] is a systematic illustration of such kind of dequantisation.

[1]This is indeed an isomorphism when $h \neq 0$.

More about Maclov Dequantisation

Intuitively, such $\odot_h$ can be extended to $\frac{1}{h}$-norm for each $h \in [0, 1]$.

If one focuses on the limit at $h = 0$ (in sense of C^0 continuity), then we have the following correspondence

$(\mathscr{F}, +, \cdot)$	$(\mathscr{F}_0, \oplus_0, \odot_0)$
$p(x) = \sum_k a_k x^k$	$M_p(u) = \max_k\{ku + \ln a_k\}$
Integral	essential supremum
$\int_X f$	$\operatorname{ess\,sup}_X\{f(x)\}$
Fourier transform	Legendre transform
$\tilde{f}(\xi) = \int e^{ix\xi} f(x) \mathrm{d}x$	$\tilde{f}(\xi) = \operatorname{ess\,sup}\{x \cdot \xi - f(x)\}$
Linear problem	Convex optimisation problem

If fact, the $\odot_h$ can be regarded as the *degraded forms* of $+$.

Patchworking on Plane Algebraic Curves

PLANE ALGEBRAIC CURVES ON $\log\log$ PAPER

Similarly, the monomial ax^ky^l with $a > 0$ under the $\log\log$ paper is a plane $w = ku + lv + \ln a$. The graph Γ_p lies in the neighbourhood of such surfaces. We can also define $\Gamma_{M(p)}$, Γ_f^h, the continuous deformation $\Gamma_{p_h}^h$ for $h \in (0, 1]$, etc..

The set of zeros $V_{Q_{++}}(p)$ is also a continuous deformation of $\Gamma_{p+} \cap \Gamma_{p-}$ projected on $S_0^2(= \mathbb{R}^2)$. In order to analysis the topology of $p(x, y)$ with digree m, one just need to consider the supremum of the set of planes $U_+ := \cup_{a^{kl}>0}\{w = ku + lv + \ln a^{kl}\}$ that derives from monomials in $p_+(x, y)$, i.e., $\{a^{kl}x^ky^l\}_{a^{kl}>0}$, as well as the $U_- := \cup_{a^{kl}<0}\{w = ku + lv + \ln(-a^{kl})\}$ from $p_-(x, y)$. The intersection of $\Gamma_{p_+} := \sup U_+$ and $\Gamma_{p_-} := \sup U_-$ is what we desired.

Visualise the Plane Algebraic Curve

We take $a(x, y) = x^3 + 2y + x + xy - (3x^2 + y^2 + 1) = 0$ as an example. The topology of $V_{Q_{++}}(a)$ is shown in **Figure 4**.

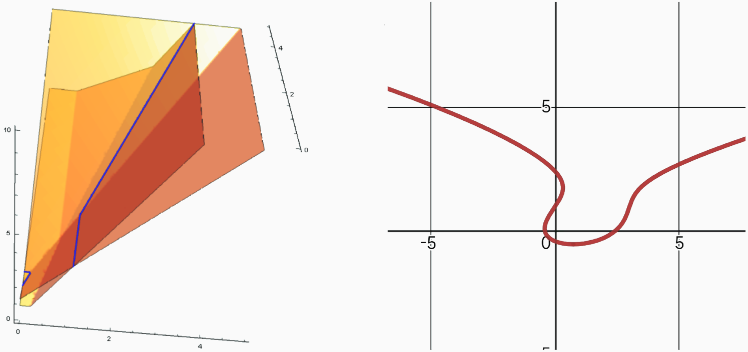

Figure 4: The $\log \log$ visualisation versus the real curve of $V_{Q_{++}}(a)$

Chart of a Polynomial

The chart of a polynomial is a set of simplicia with codimension 1 on the components of a Newton polygon[2] $\Delta(a)$. The chart on a given quadrant Q is homeomorphic (or homotopic for degenerated cases) to $V_Q(p)$.

Especially for degenerated cases, the Newton polygon of a non-singular quasi-homogeneous polynomial[3] is a line, e.g. **Figure 5**.

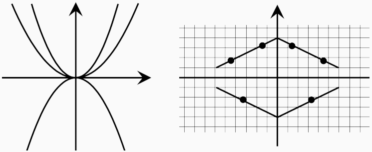

Figure 5: The Newton polygon and charts of $a(x, y) = (x^2 - y)(x^2 + y)(2x^2 - y)y$

The $\log\log$ paper is a set of parallel lines perpendicular to $\Delta(a)$.

[2]Newton polygon $\Delta(a)$ of $a = a(x, y)$ is the convex hull of $\{(l, k) : a_{k,l} \neq 0\}$ for $a(x, y) = \sum_{0 \leq k+l \leq m} a_{k,l} x^k y^l$.
[3]which is in forms of $a(x, y) = \sum_{i=0}^{k} \alpha_i x^{pi+p_0} y^{q(k-i)+q_0}$.

Chart of a Non-quasi-homogeneous Polynomial

We first consider the charts of non-quasi-homogeneous trinomial $8x^3 - x^2 + 4y^2$ shown in **Figure 6**.

For simplicity, let the charts be the mid-segments. Here the signs are deliberately marked to distinguish the connected components.

One can verify that such construction fits all trinomials.

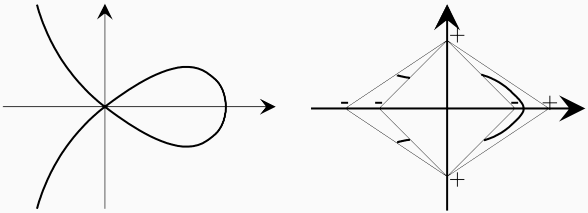

Figure 6: The charts of $8x^3 - x^2 + 4y^2$ on each quadrant.

Chart of a Non-quasi-homogeneous Polynomial

Consider a set of real trinomials $\{a_k(x, y)\}_{k=1}^{s}$, provided that

$$[\mathrm{Int}\Delta(a_i)] \cap [\mathrm{Int}\Delta(a_j)] = 0, \text{ whence } i \neq j. \tag{8}$$

We suppose that the coefficients of $x^k y^l$ in $\{a_r : (k, l) \in \Delta(a_r)\}$ are the same, so that $a = \cup_{k=1}^{s} a_k$ is well-defined.

Let $\nu : \Delta(a) \to \mathbb{R}$ be such that

- ν are piecewise linear on $\Delta(a)$, while not linear on the union of any pairs of different triangles.
- $\nu : \Delta(a) \cap \mathbb{Z}^2 \to \mathbb{Z}$.

Prerequisites of Patchworking Theorem

- Patchworking for trinomials,
- The bonding lemma for set of disjoint trinomials.

Construct Patchworking Segments in $\overline{Q_{++}}$

The initial data for patchworking in $\overline{Q_{++}}$ includes several steps as follows

- m, the degree of the polynomial,
- Δ, the Newton polygon[4],
- $\{\sigma_{k,l} \in \{\pm 1\} : (k,l) \in \overline{\Delta}\}$.
- τ, the convex triangulation of Δ with vertices in integer coordinates,
- $\nu : \Delta \to \mathbb{R}_+$, a piecewise linear function which is not linear on the union of any two triangles.

For instance, the patchworking of a conic with given $m = 2$, triangulation τ, and $\{\sigma_{k,l}\}$ in $\overline{Q_{++}}$ is shown in the first plot of **Figure 7**.

[4] The convex hull of $\{(0,0), (0,m), (m,0)\}$ is commonly utilised.

Procedure for Constructing Patchworking Segments

The basic procedure for constructing the patchworking segments (L, Δ) includes:

1. Construct $(L, \overline{Q_{++}})$ with initial values.
2. Reflect Δ as well as the triangulation τ with x and y axes.
3. Extend the sign function onto Δ_*[5] in the light of

$$\sigma_{\varepsilon i, \delta j} = \begin{cases} \sigma_{i,j} & \|(i,j) - (\varepsilon i, \delta j)\|_1 = 4k, \\ -\sigma_{i,j} & \|(i,j) - (\varepsilon i, \delta j)\|_1 = 4k + 2. \end{cases} \tag{9}$$

4. Whence a triangle in the triangulation τ has vertices of different signs, draw mid-segment(s) separating pluses from minuses.
5. Let L be the union of all segments constructed in the previous step. Then (Δ_*, L) is called the result of combinatorial patchworking (shown in **Figure 7**).

[5] We denote $\Delta_* := \cup_{\varepsilon,\delta \in \{\pm 1\}} \Delta_{\varepsilon,\delta}$

BLANK

The corresponding one-parameter family of polynomials on affine plane $\mathbb{A}^2_{\mathbb{R}}$ is shown as

$$b_t(x, y) = \sum_{(k,l)\in\mathcal{V}(\tau)} \sigma_{k,l} \cdot t^{\nu(k,l)} \cdot x^k y^l. \tag{10}$$

Q: Does $b_t(x, y)$ has the same topology as the segments?

This is true when $t \to 0^+$.

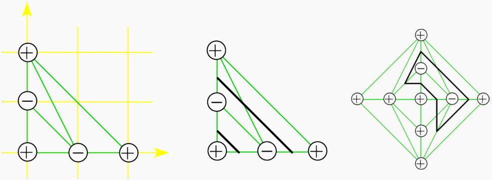

Figure 7: Patchwork a conic in $\mathbb{A}^2_{\mathbb{R}}$

Main Theorem: Patchworking Theorem

Patchworking theorem There exists $t_0 > 0$ such that for any $t \in (0, t_0]$ the equation $b_t(x, y) = 0$ defines in the plane c_t a curve such that the pair $(\mathbb{A}^2_{\mathbb{R}}, c_t)$ is homeomorphic to the pair (Δ_*, L).

The equation $B_t(x_0, x_1, x_2)$ defines in the real projective plane $\mathbb{P}^2_{\mathbb{R}}$ a curve C_t such that $(\mathbb{P}^2_{\mathbb{R}}, C_t)$ is homeomorphic to $(\overline{\Delta}_*, L)$.

Remark:

- $B_t(x_0, x_1, x_2) = \sum_{(k,l)\in\mathcal{V}(\tau)} \sigma_{k,l} \cdot t^{\nu(k,l)} \cdot x_0^{m-k-l} x_1^k x_2^l$ on $\mathbb{P}^2_{\mathbb{R}}$ is the homeogeneous form of $b_t(x, y) = \sum_{(k,l)\in\mathcal{V}(\tau)} \sigma_{k,l} \cdot t^{\nu(k,l)} \cdot x^k y^l$ on $\mathbb{A}^2_{\mathbb{R}}$.
- c_t (or C_t) is the set of zeros $V_{\mathbb{A}^2_{\mathbb{R}}} b_t$ (or $V_{\mathbb{P}^2_{\mathbb{R}}} B_t$).

Hilbert’s 16th Problem

Introduction to Hilbert's 16th Problem

Harnack (1876) prove that the number of components of a real projective curve of degree m is at most $\binom{m-1}{2} + 1$. We call a curve **M-curve** whenever the equality holds.

The first part of Hilbert's 16th problem is **to describe which real schemes of ovals can be realised by a real algebraic curve of degree m**. The full classification M-curve of degree 6 is shown in **Figure 8**.

Figure 8: Topology of M-curve of degree 6.

Harnack's Construction

Harnack's construction is to

1. Perturbs the union of a line and a circle.
2. Combined the result curve with the previous line for a new perturbation.
3. And so forth...

A Harnack curve of degree $2k$ has

- $p = 3\binom{k}{2} + 1$ outer ovals,
- $n = \binom{k-1}{2}$ inner ovals.

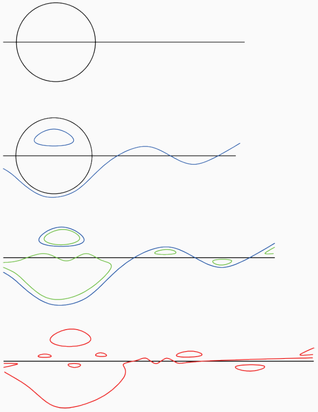

Figure 9: The idea of Harnack's construction.

Harnack Distribution

In the light of Harnack's construction, the sign distribution $\sigma_{k,l}$ in $\overline{Q_{++}}$ takes minus only on even grids, i.e., **Figure 10**.

We utilise the symbol in [4] to denote such scheme by $\langle 9 \amalg 1\langle 1\rangle\rangle$.

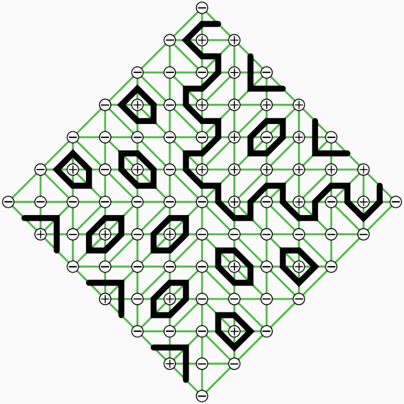

Figure 10: Harnack's sign distribution for $m = 6$.

Hilbert's Construction

Hilbert's construction begin with the union of two ellipses...

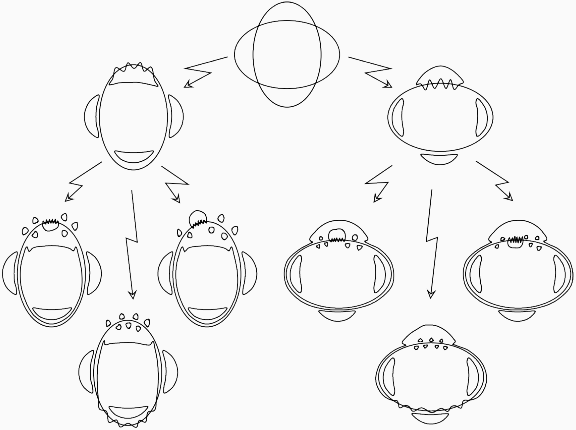

Figure 11: The idea of Hilbert's construction.

Gudkov's Eureka

The preexisting schemes are coloured black in **Figure 12**. In order to make it more symmetric, Gudkov (1971) found the final answer.

$$\langle 9 \amalg 1\langle 1\rangle\rangle \qquad \langle 5 \amalg 1\langle 5\rangle\rangle \qquad \langle 1 \amalg 1\langle 9\rangle\rangle$$

$$\langle 10\rangle \quad \langle 8 \amalg 1\langle 1\rangle\rangle \qquad \langle 5 \amalg 1\langle 4\rangle\rangle \quad \langle 4 \amalg 1\langle 5\rangle\rangle \qquad \langle 1 \amalg 1\langle 8\rangle\rangle \quad \langle 1\langle 9\rangle\rangle$$

$$\langle 9\rangle \quad \langle 7 \amalg 1\langle 1\rangle\rangle \quad \langle 6 \amalg 1\langle 2\rangle\rangle \quad \langle 5 \amalg 1\langle 3\rangle\rangle \quad \langle 4 \amalg 1\langle 4\rangle\rangle \quad \langle 3 \amalg 1\langle 5\rangle\rangle \quad \langle 2 \amalg 1\langle 6\rangle\rangle \quad \langle 1 \amalg 1\langle 7\rangle\rangle \quad \langle 1\langle 8\rangle\rangle$$

$$\langle 8\rangle \quad \langle 6 \amalg 1\langle 1\rangle\rangle \quad \langle 5 \amalg 1\langle 2\rangle\rangle \quad \langle 4 \amalg 1\langle 3\rangle\rangle \quad \langle 3 \amalg 1\langle 4\rangle\rangle \quad \langle 2 \amalg 1\langle 5\rangle\rangle \quad \langle 1 \amalg 1\langle 6\rangle\rangle \quad \langle 1\langle 7\rangle\rangle$$

$$\langle 7\rangle \quad \langle 5 \amalg 1\langle 1\rangle\rangle \quad \langle 4 \amalg 1\langle 2\rangle\rangle \quad \langle 3 \amalg 1\langle 3\rangle\rangle \quad \langle 2 \amalg 1\langle 4\rangle\rangle \quad \langle 1 \amalg 1\langle 5\rangle\rangle \quad \langle 1\langle 6\rangle\rangle$$

$$\langle 6\rangle \quad \langle 4 \amalg 1\langle 1\rangle\rangle \quad \langle 3 \amalg 1\langle 2\rangle\rangle \quad \langle 2 \amalg 1\langle 3\rangle\rangle \quad \langle 1 \amalg 1\langle 4\rangle\rangle \quad \langle 1\langle 5\rangle\rangle$$

$$\langle 5\rangle \quad \langle 3 \amalg 1\langle 1\rangle\rangle \quad \langle 2 \amalg 1\langle 2\rangle\rangle \quad \langle 1 \amalg 1\langle 3\rangle\rangle \quad \langle 1\langle 4\rangle\rangle$$

$$\langle 3\rangle \quad \langle 1 \amalg 1\langle 1\rangle\rangle \quad \langle 1\langle 2\rangle\rangle \qquad \langle 1\langle 1\langle 1\rangle\rangle\rangle$$

$$\langle 2\rangle \quad \langle 1\langle 1\rangle\rangle$$

$$\langle 1\rangle$$

$$\langle 0\rangle$$

Figure 12: Schemes of curves with degree 6.

Ragsdale Conjecture

Ragsdale (1906) observed that

- for any Harnack's M-curve of even degree $m = 2k$, we have $p = 3\binom{k}{2} + 1$ and $n = \binom{k-1}{2}$.
- for any Hilbert's M-curve of even degree $m = 2k$, we have $\binom{k-1}{2} + 1 \leq p \leq 3\binom{k}{2} + 1$, $\binom{k-1}{2} \leq n \leq 3\binom{k}{2}$.

It motivates the following conjecture by Ragsdale, that is,

Ragsdale's conjecture

For any curve of even degree $m = 2k$, one has $p \leq 3\binom{k}{2} + 1$, and $n \leq 3\binom{k}{2}$.

The Counterexample of Ragsdale's Conjuncture

It is proved by Oleg [2] that

- there exists a nonsingular real algebraic plane curve of degree $2k$ with
$$p = \frac{3k(k-1)}{2} + 1 + \left[\frac{(k-3)^2+4}{8}\right]. \tag{11}$$
- there exists a nonsingular real algebraic plane curve of degree $2k$ with
$$n = \frac{3k(k-1)}{2} + \left[\frac{(k-3)^2+4}{8}\right]. \tag{12}$$

Tessellation of $\langle 1 \langle 2 \rangle \rangle$ Hexagon

Consider the patchworking of the hexagon in **Figure 13** and the *tessellation* in $\Delta(x^m + y^m + 1)$ in **Figure 14**.

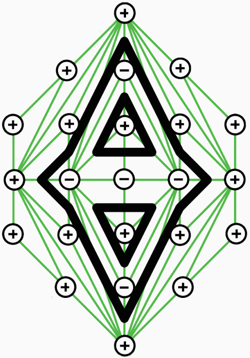

Figure 13: $\langle 1 \langle 2 \rangle \rangle$ hexagon.

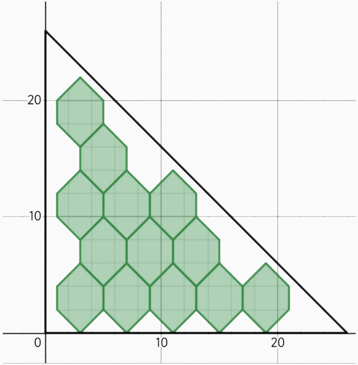

Figure 14: The hexagon tessellation.

Counterexample of Ragsdale's conjecture p

For the partition from tessellation of $\langle\, 1\langle\, 2\,\rangle\rangle$ hexagons, we apply the Harnack's distribution to the uncovered vertices in $\overline{Q_{++}}$. We denote the number of hexagons in $\Delta(x^{2k}+y^{2k}+1)$ by

$$\alpha := \left\lfloor \frac{(k-3)^2+4}{8} \right\rfloor. \tag{13}$$

Then the real scheme outcomes

$$\langle (3\binom{k}{2}-\alpha) \amalg 1\langle (\binom{k-1}{2}-4\alpha) \amalg \alpha\langle 2\rangle\rangle\rangle. \tag{14}$$

It yields that the number of even ovals is

$$p = 3\binom{k}{2} + 1 + \alpha = \frac{3k(k-1)}{2} + 1 + \left\lfloor \frac{(k-3)^2+4}{8} \right\rfloor. \tag{15}$$

Counterexample of Ragsdale's conjecture on n

As shown in **Figure 15**, we adjust the the signs and triangulation in pleural region of the previous counterexample.

- hexa-tessellation
- pleural region
- sign distribution
- triangulation

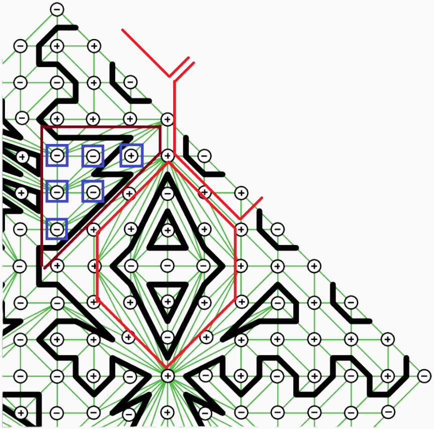

Figure 15: Adjustment in Q_{++}.

Counterexample of Ragsdale's conjecture on n

The patchworking in the previous page yields the real scheme

$$\langle 1 \langle 3\binom{k}{2} - \alpha \rangle \amalg \alpha \langle 2 \rangle \amalg (\binom{k-1}{2} - 4\alpha - 1) \rangle. \tag{16}$$

It yields that the number of even ovals is

$$p = 3\binom{k}{2} + \alpha = \frac{3k(k-1)}{2} + \left\lfloor \frac{(k-3)^2+4}{8} \right\rfloor. \tag{17}$$

Improved upper bounds for counterexamples

The improved upper bound [1] of p is presented below

$$p = 3\binom{k}{2} + 1 + \left\lfloor \frac{k^2 - 7k + 16}{6} \right\rfloor.$$

A counterexample for n of degree 10

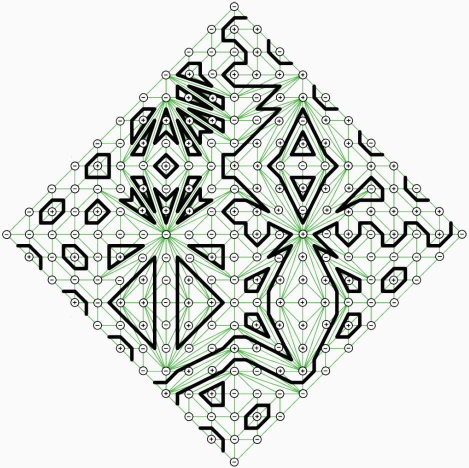

Figure 16: Scheme $\langle 1\langle 29\rangle \amalg 1\langle 2\rangle \amalg 1\rangle$

References I

B. Haas.
Les multilucarnes: nouveaux contre-exemples à la conjecture de Ragsdale.
C. R. Acad. Sci. Paris Sér. I Math., 320(12):1507–1512, 1995.

I. Itenberg and O. Viro.
Patchworking algebraic curves disproves the ragsdale conjecture.
The Mathematical Intelligencer, 18(4):19–28, Sep 1996.

V. N. Kolokoltsov and V. P. Maslov.
Idempotent Analysis and Its Applications.
Springer Netherlands, 1997.

J. Li.
Hilbert's 16th problem and bifurcations of planar polynomial vector fields.
Int. J. Bifurc. Chaos, 13:47–106, 2003.

G. L. Litvinov.
The maslov dequantization, idempotent and tropical mathematics: A brief introduction, 2005.

O. Viro.
Patchworking real algebraic varieties, 2006.

Thanks for listening!